Towards a Flying Assistant Paradigm: the OTHex

Nicolas Staub, Davide Bicego, Quentin Sablé, Victor Arellano-Quintana,
Subodh Mishra, Antonio Franchi

▶ **To cite this version:**

HAL Id: hal-01716845
https://laas.hal.science/hal-01716845

Submitted on 24 Feb 2018

Towards a Flying Assistant Paradigm: the OTHex

Nicolas Staub[1†], Davide Bicego[1†], Quentin Sablé[1], Victor Arellano[1,2], Subodh Mishra[1] and Antonio Franchi[1]

Abstract— This paper presents the OTHex platform for aerial manipulation developed at LAAS–CNRS. The OTHex is probably the first multi-directional thrust platform designed to act as Flying Assistant which can aid human operators and/or Ground Manipulators to move long bars for assembly and maintenance tasks. The work emphasis is on task-driven custom design and experimental validations. The proposed control framework is built around a low-level geometric controller, and includes an external wrench estimator, an admittance filter, and a trajectory generator. This tool gives the system the necessary compliance to resist external force disturbances arising from contact with the surrounding environment or to parameter uncertainties in the load. A set of experiments validates the real-world applicability and robustness of the overall system.

Fig. 1: CAD view of the Open-Tilted Hexarotor (OTHex) designed and developed at LAAS-CNRS.

I. INTRODUCTION

In the recent years, the topic of *Aerial Physical Interaction* (APhI) and particularly of *Aerial Manipulation* (AM) has gained significant interest in the robotics and control community. Recent achievements are supported by strong control results for under-actuated *Vertical Take-Off and Landing* (VTOL) vehicles and the relatively cheap acquisition and maintenance costs for small/lightweight robots of this kind. Research effort on AM studies aerial vehicles equipped with one or more robotic arms, allowing to describe those systems as *Aerial Robots* (ARs). This research line has been particularly fostered by European projects like ARCAS, AeroArms, and AeroWorks[1], leading to results in mechanical design of new aerial platforms [1], [2], control analysis [3], [4] visual perception for AM [5], [6], and planning [7], [8]. The literature also encompasses the use of VTOLs to transport loads and interact by means of cables, see [9]–[11] and references therein. However, the limited payload of small ARs limits the number of real life applications.

On the other hand, there are many real cases in which only a part of the whole object has to be substantially lifted from the ground, while another part can (or has to) remain close to it. Tasks like assembly, maintenance or decommissioning involving the manipulation of long bars are concrete examples of such cases. As an illustration of such tasks, one can think about gutters and pipes installation, cropping fruits or trimming trees using a pole saw. Therefore it is worth to focus the efforts on an approach where the load
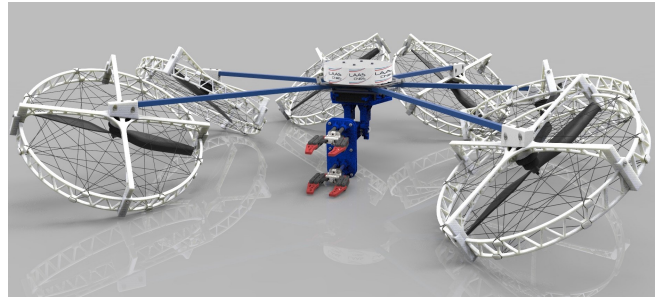
is mainly carried by a ground robot or a human operator helped by one or more ARs [12] used as *Flying Assistants*.

A ground robot or a human operator handling a long bar by one of its ends have to face the following challenges: *i)* high torque at the grasping point, *ii)* reduced dexterity in the manipulation and *iii)* vibrations of the bar and its other end. All three can be mitigated by using Flying Assistants.

In this paper we present an in-house developed AR that can help lifting bars. Differently from [12], we propose a solution with a *multi-directional thrust* flying vehicle, in order to better resist lateral perturbations and simplify the decoupling mechanism for the load-induced torque. Relying on the experience in analyzing, designing and controlling multi-directional thrust platforms shown in our previous works [2], [13]–[15], we developed a novel Flying Assistant, called *Open-Tilted Hexarotor* (OTHex), shown in Figs. 1 and 5, where is clearly visible the extra-aperture that lets a bar pass through. The low-level control framework is based on the one presented in [13], [14], on top of which a dedicated trajectory generator is implemented for the bar lifting task.

In the experimental section, we demonstrate the performances of the OTHex for lifting bars (control, stabilization), thanks to its tailored design. Moreover, the robustness of the controller to external perturbations and parameter uncertainties is validated, with results demonstrating the OTHex promising capabilities as a Flying Assistant for cooperative manipulation with either a ground robot or a human operator.

The rest of the paper is organized as follows, Sec. II outlines the idea behind the design process of the OTHex, the modeling and the control architecture are then presented in Sec. III and Sec. IV, respectively. Emphasis is put on the experiments, with an in-depth presentation of the experimental setup in Sec. V and a discussion on the results in Sec. VI.

[1]LAAS–CNRS, Université de Toulouse, CNRS, Toulouse, France, antonio.franchi@laas.fr
[2]ESIME-UA, National Polytechnic Institute, Mexico City, Mexico
† Both authors contributed equally to this work.
[1]http://www.arcas-project.eu/, https://aeroarms-project.eu/, https://www.aeroworks2020.eu/.
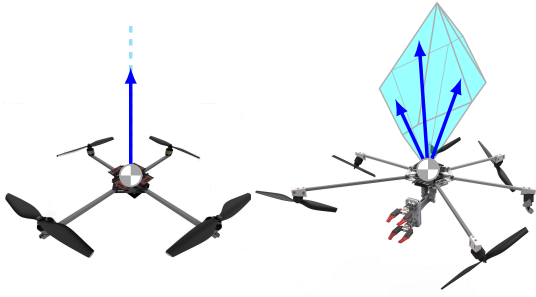
Fig. 2: Possible thrust direction based on collinear (left) and tilted propellers design (right). Highlighted in cyan the set of possible forces when the requested moment is zero, with three examples inside the polytope for the multi-directional thrust case.
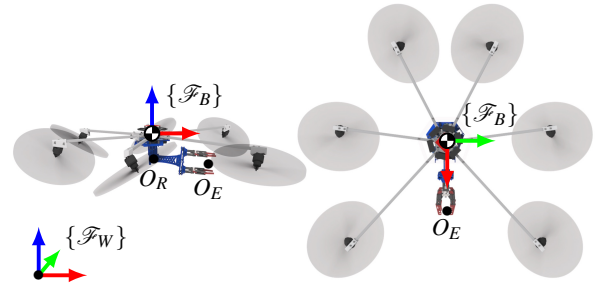

Fig. 3: Side view (left) and top view (right) of the OTHex in CAD, with the key modeling parameters super-imposed. In particular the aperture in the propeller distribution is clearly visible in the top view, while the propeller tilting in the lateral view.

Finally, Sec. VII presents the direction of our future work.

II. DESIGN CONSIDERATIONS

In typical VTOL platforms all the propellers, responsible for the robot actuation, spin about parallel directions, i.e., they are collinear. The thrust force generated by each propeller is directed along the same line and therefore the total force is exerted along that unique fixed direction in body frame, see Fig. 2 (left). To follow an arbitrary 3D position trajectory the robot has to modify its orientation in order to re-orient the thrust direction at every instant in accordance with the needed acceleration. This fact makes collinear-rotor VTOLs underactuated. Their translational and rotational dynamics are directly coupled, hence tracking arbitrary 6D reference trajectory is impossible. Physical interaction with such platforms is challenging and suboptimal, see e.g., [16] and references therein.

In the design of the OTHex the propeller rotation axes are tilted in different directions. This allows to exert the thrust inside a polytope, see Fig. 2 (right), by just changing the control input allocation, thus turning the platform from underactuated (uni-directional thrust) to fully actuated (multi-directional thrust). This design has been introduced earlier in our previous works [2] [17]. The major design novelty of this paper is the reasoning leading to an aperture in the propeller volume, discarding more trivial solutions in favor of a significant system complexity reduction.

One mechanical challenge during aerial manipulation is to prevent collision between the manipulated load and the spinning propellers. This issue is easily handled when manipulated objects can remain at a safe distance under the volume occupied by the spinning propellers, but it cannot for more complex tasks such as bar lifting.

An approach to handle long bars is to use a robotic arm with a workspace large enough to handle the bar outside of the platform perimeter. This approach costs an increased weight and a decreased bar payload. Furthermore, when the arm extends, the force disturbances from the load side may generate large destabilizing moments on the AR.

To tackle this issue, we designed the OTHex, with a non-regular frame arrangement, introducing a consistent aperture between the two front propellers, hence the denomination

Open. In order to compensate for the non-regular location of the propellers and the shift of Center of Mass (CoM) of the total platform, w.r.t. a regular arrangement, the two frame elements delimiting the aperture are longer than the others. This ensures that in contact-free hovering the control effort is equally distributed between the six propellers.

Thanks to the ability to exert a multi-directional thrust, the OTHex does not need an actuated arm. Thus, a mechanically simpler 1-DoF passive arm can be used to perform complex and dexterous manipulation tasks. The full actuation allows both the system complexity reduction and the weight/payload decrease/increase, respectively.

III. MODELING

We consider as AR a multi-directional thrust flying platform equipped with a passive 1-DoF arm. The presented framework is generic and independent w.r.t. the arm dimensions, and the flying platform design, as long as it allows multi-directional thrust actuation.

Let us denote with $\mathscr{F}_W$ the inertial world frame, and its origin and major axes by $O_W - \{\mathbf{x}_W, \mathbf{y}_W, \mathbf{z}_W\}$, respectively, see Fig. 3. The body frame, rigidly attached to the robot, is denoted $\mathscr{F}_B : O_B - \{\mathbf{x}_B, \mathbf{y}_B, \mathbf{z}_B\}$, where O_B coincides with the CoM of the flying platform + base of the arm. The position of O_B in $\mathscr{F}_W$ is denoted by $\mathbf{p}_B \in \mathbb{R}^3$. The points O_R and O_E are the center of rotation of the passive joint and the Tool Center Point on the end-effector, respectively. The distances $O_B O_R$ and $O_R O_E$ are denoted d_1 and d_2 respectively.

Using the Netwon-Euler formalism, the AR dynamics are

$$\begin{bmatrix} m\ddot{\mathbf{p}}_B \\ \mathbf{J}\dot{\boldsymbol{\omega}}_B \end{bmatrix} = - \begin{bmatrix} mg\mathbf{z}_W \\ \boldsymbol{\omega}_B \times \mathbf{J}\boldsymbol{\omega}_B \end{bmatrix} + \text{diag}(\mathbf{R}_B, \mathbf{I})\,\mathbf{F}\boldsymbol{u} + \mathbf{J}_R^T \mathbf{w}_R, \quad (1)$$

with m and $\mathbf{J} \in \mathbb{R}^{3\times3}$ respectively denoting the AR mass and its moment of inertia w.r.t. O_B and expressed in $\mathscr{F}_B$. The term $-g\mathbf{z}_W$ is the gravitational acceleration. Moreover $\boldsymbol{u} = [u_1 \cdots u_6]^T$ is the control input vector of the six squared propeller spinning velocities, $\mathbf{F}$ is the control allocation matrix, a function of the physical properties of the AR (i.e., propellers spatial distribution and tilting angles, and thrust/drag coefficients, see [2]). The rotation matrix $\mathbf{R}_B \in SO(3)$ represents the orientation of the AR frame $\mathscr{F}_B$ in
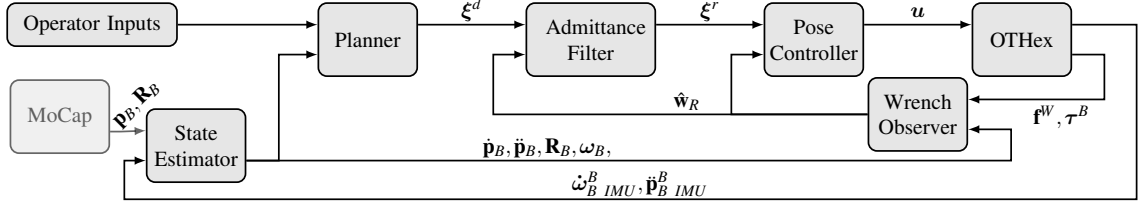
Fig. 4: Block-diagram of the full control architecture implemented for the OTHex. The symbol $\boldsymbol{\xi} = (\mathbf{p}_B, \dot{\mathbf{p}}_B, \ddot{\mathbf{p}}_B, \mathbf{R}_B, \boldsymbol{\omega}_B, \dot{\boldsymbol{\omega}}_B)$ is a compact notation for the full state of the system, superscripts ^{d} and ^{r} denote the desired and the reference trajectory, respectively. The state estimator is fed with pose measurements, in our case by a MoCap, which can be replaced by a visual pose estimator when a MoCap is not available.

the world frame, $\mathscr{F}_W$. The external wrench arising at O_R expressed in $\mathscr{F}_W$ is denoted by $\mathbf{w}_R \in \mathbb{R}^6$, hence the transposed Jacobian $\mathbf{J}_R^T$ maps the wrench at O_R to the one at O_B. We chose to consider the point O_R for the wrench estimator because it remains fixed in body-frame $\mathscr{F}_B$, unlike O_E. Moreover, once the gripper is attached to the bar it is preferable to consider a unique rigid body {bar+gripper} applying forces to the OTHex, saving the use of a more complex model in the wrench estimator.

IV. CONTROL ARCHITECTURE

This section highlights the main components of the control architecture, which have been detailed in [14] and will only be outlined here for sake of completeness. The control architecture is composed of four main parts: *1)* a low-level pose controller, *2)* a wrench observer, *3)* an admittance filter, and *4)* a high-level planner, plus several peripheral components necessary to feed the above components with the system information, see Fig. 4.

1) Low-level Pose Controller: The Pose Controller is made by three stages. The first stage gets as input the reference pose (position plus orientation) producing as output a reference control force $\mathbf{f}^r \in \mathbb{R}^3$ and a desired feasible orientation $\tilde{\mathbf{R}}_B^r$ (a priori different from the reference one). The actuators limits are accounted for in this computation, in fact $\tilde{\mathbf{R}}_B^r$ minimizes the distance to $\mathbf{R}_B^r$ in $SO(3)$ while keeping $\mathbf{f}^r$ inside the actuation limits (the polytope shown in Fig. 2, right). The second stage computes a reference control torque $\boldsymbol{\tau}^r \in \mathbb{R}^3$ to track the desired rotation $\tilde{\mathbf{R}}_B^r$ provided by the first stage. The final stage computes the actual propeller spinning velocity $\boldsymbol{u}$ in order to generate $\mathbf{f}^r$ and $\boldsymbol{\tau}^r$. This controller has been detailed in [2], [13] and is used here as a basis.

2) Wrench Observer: The wrench observer is based on a dynamic model of the wrench generated by the propellers, in particular it contains an identified model of the aerodynamic effects at play and of the geometrical model of the AR. Via the expression of the OTHex dynamics in the Lagrangian form, a generalized momentum observer is designed, as presented in [14], [18]. This results in the expression of $\hat{\mathbf{w}}_R$ as the output of a first order low-pass dynamic system.

3) Admittance Filter: In order to perform safe physical interactions with the environment, a compliant behavior of the AR should be ensured. Denote with $(\mathbf{p}_R^d, \mathbf{R}_R^d, v_R^d, \dot{v}_R^d)$ the desired trajectory of the interaction point, i.e., O_R. This

reference is given by a trajectory planner and represents the input of the admittance filter. The admittance filter computes a new reference trajectory $(\mathbf{p}_R^r, \mathbf{R}_R^r, v_R^r, \dot{v}_R^r)$ mimicking the dynamics of a 6-DoF mass-spring-damper system. Its inertia, damping and stiffness matrices, all positive-definite, are chosen to enforce an over-damped behavior of the system, thus granting the stability of the AR when in contact with the environment. The admittance filter generates a reference trajectory for O_R, which will be turned into a trajectory for O_B using direct and differential rigid body equations.

4) High-level planner: For our experimental purpose a planner was devised, composed of: *i)* a task planner, *ii)* a Finite State Machine (FSM), and *iii)* a trajectory generator with a different policy for each state of the FSM. It generates the reference state and nominal force trajectory to be followed by the OTHex and also triggers the grippers and control/warning lights of the OTHex, easing system state monitoring for the operator. The FSM allows to switch trajectory generation policies for contact and contactless operations.

V. EXPERIMENTAL SETUP

The OTHex, see Fig. 5, has a total mass of $m = 2.48\,\mathrm{kg}$ for a 0.8 m span. The vertical distance between the CoM of the flying platform and the passive joint center is $d_1 = 0.068\,\mathrm{m}$. The principal components of the inertia tensor have been obtained via a detailed CAD model and $\mathbf{J} = \mathrm{diag}\,(0.124\ 0.110\ 0.192)\,\mathrm{kg\,m}^2$. Other significant parameters are listed in Tab. I. The flying platform is composed of a rigid structure made by six aluminum bars and a central plate, for mechanical robustness and ease of maintenance. The actuation units, located at the end of each bar, are composed of a MK3638 brushless motor from MikroKopter and 12" propellers with 4.5" pitch, each developing a maximum thrust of about 12 N. They are fixed via 3D-printed adapters in order to provide the necessary tilting angles, see Fig. 3 and Fig. 5, for the multi-directional thrust ability. The propeller tilting angles are $|\alpha| = 35°$ and $\beta = -10°$ (see [2] for their definition), which guarantees a well-balanced choice between maximum lateral forces and losses due to internal forces in contactless hovering.

The electronics is composed of six electronic speed controllers (ESC) BL-Ctrl-2.0 from MikroKopter, running an in-house developed firmware that performs closed-loop spinning frequency control and accepts desired spinning frequency at 1 kHz [19]. This allows a fine control of the
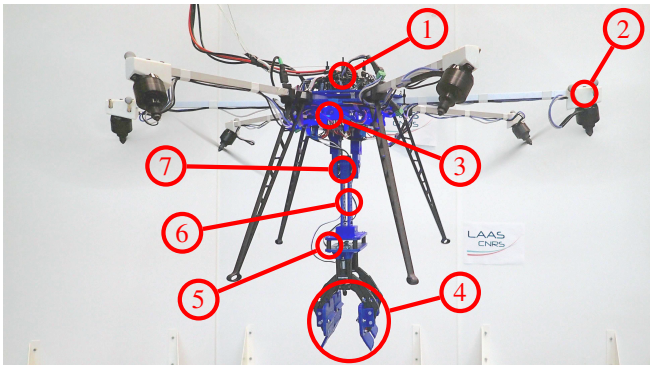
Fig. 5: Back view of the OTHex with; flight electronics (1), tilting adapters (2), gripper electronics (3), claws (4), extra dampers for compliance (5), and arm (6) mounted on the passive joint (7).

Parameter	Value	Units
OTHex total weight (without battery)	2.48	[kg]
passive arm total weight	0.406	[kg]
arm top part weight	0.115	[kg]
arm gripper part weight	0.291	[kg]
frontal aperture angle	85	[°]
max diameter of the grasped bar	0.25	[m]
extra admissible payload	2.9	[kg]
propeller 1st tilt angle: $|\alpha|$	35	[°]
propeller 2nd tilt angle: β	-10	[°]
max. lateral admissible force (hovering)	8	[N]

TABLE I: OTHex main characteristics.

propeller spinning velocity, coupled with a static map of the force and moment produced at a given spinning velocity, it results in a precise force control of the platform. It also provides, at the same rate, measurements of the current spinning frequency that is used by the wrench observer.

Below the flying platform, a 1-DoF passive manipulator is fixed. It is composed of a passive revolute joint, a 3D-printed arm, of parameter $d_2 = 0.248$ m and a set of two Makeblock robotic grippers. The base of the manipulator is a 3D-printed structure, also serving as electronics and battery case, and is mounted directly on the central plate of the flying platform. The grippers have been chosen for their lightweight and easy integration characteristics. The gripper electronics is composed of an Arduino Nano board and some power converters, encased in the 3D-printed structure.

Additionally, as pose sensor, we use an external motion capture system (Optitrack MoCap) based on optical markers. Its pose measurement (120 Hz) are fused with the IMU measurements (1 kHz) using an UKF based state estimator, thus obtaining a full state estimate at 1 kHz. It has been shown empirically that the state estimator performs well even with pose measurement coming from the MoCap at 30 Hz.

VI. EXPERIMENTAL RESULTS

For the experiments, we investigate the lifting of a metal bar, of weight 1.27 kg and length 1.45 m, from an horizontal to a vertical position. This action can be seen as mimicking,

at a lower scale, a structure construction or a gutter installation. In our setup the bar is rigidly attached to the ground via passive revolute joint to prevent slipping.

1) Experiment in Nominal Conditions: In a first experiment, we perform a nominal bar lift, from a rest angle of $\theta_0 = 0$ to a final angle of $\theta_f = \pi/2$, as depicted in Fig. 6 which highlights the important stages in the motion. In this experiment the contactless flight is commanded manually by a human operator, to reach the desired grasping point. Since there should be no physical interaction with the environment, the admittance filter is turned off until the lifting phase starts. Once the contact has been established, a change of the state in the FSM is triggered to toggle the autonomous bar lifting, in which the planner provides a desired trajectory and nominal force to lift the bar, computed based on the bar kinematics. The admittance filter becomes active.

Associated results for the nominal case are presented in Fig. 7. In particular, measured quantities are in solid lines, while the desired trajectory from the planner is dotted and the compliant reference trajectory from the admittance filter is dashed. The low-level controller is fed by the dotted trajectory in free-flight and by the dashed trajectory when the admittance filter is running in contact phase. The attitude tracking is detailed in the second plot from the top, with the same convention for the lines. The third plot from top displays the desired and the measured altitude angle of the bar. It can be seen that the actual angle is behind the desired when the OTHex lifts the bar, and in advance when the bar is descending. This can be explained by the fact that the bar position (i.e., the planar trajectory) is not the regulated quantity, since the admittance filter is generating a compliant reference trajectory based on the external wrench. Therefore, the OTHex has a less aggressive behavior lifting the bar while is pulled down by the descending bar. Finally, the bottom plot shows the external wrench estimated against the nominal lift force computed by the planner. Note at the beginning of the experiment the OTHex rest on the landing platform, hence the wrench estimator senses a force along $\mathbf{z}_B$ of about 20 N (due to its weight), which vanishes as the OTHex takes off.

2) Experiments in Non-nominal Conditions: Two additional experiments intend to show the system robustness in case of : 1) parameter uncertainties about the bar physics in the planner and 2) blocked bar, to highlight the compliant behavior induced by the admittance filter.

We first induce parameter uncertainty by introducing a 20 cm bias in the grasping location of the bar in the planner. In this way the planner computes a reference trajectory for the OTHex which is unfeasible, as it is rigidly attached to the bar 20 cm away from the point considered by the planner. If this trajectory was directly sent to the pose controller, it would result in unstable behavior of the system, most likely leading to destruction. The presence of the admittance filter is then extremely important, since it modifies the nominal trajectory given by the planner, using the information of the estimated external wrench, to produce a feasible trajectory. The results of this test are gathered in Fig. 8, where we focus

(1)   (2)   (3)   (4)

Fig. 6: Time-lapse of the OTHex in the bar lifting experiment, from left to right; (1) contact free-flight, (2) grasping the horizontal bar, (3) lifting the bar, (4) bar just lifted, inverting the motion.
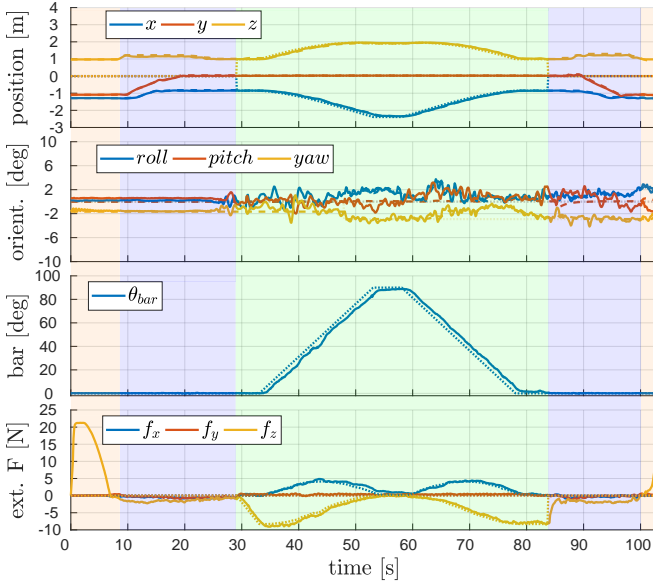

Fig. 7: Experimental data of a nominal bar lift. From top to bottom, the OTHex position and orientation, the bar tilting angle and the wrench observer forces. Quantities are denoted as follow; measured (solid), from the planner (dotted), from the admittance filter (dashed). The admittance filter is activated only during the lifting phase (green). In the contact-free flight phase (blue) the OTHex tracks a trajectory given by the planner. The moment the OTHex rests on the landing platform is colored in orange.
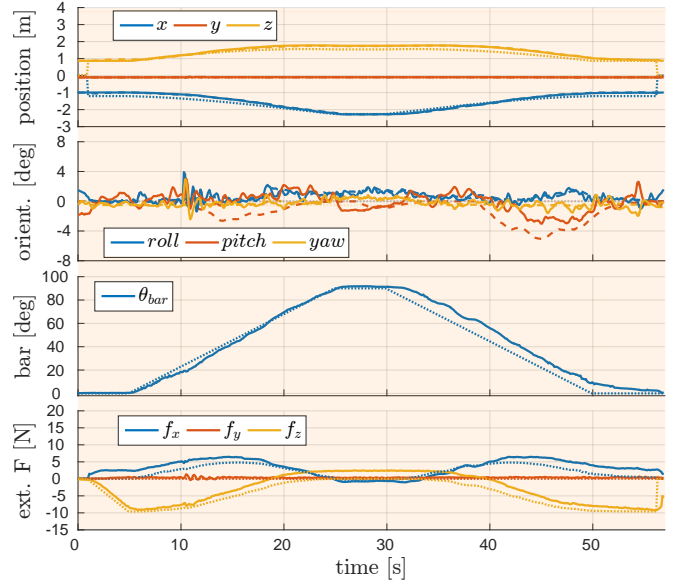
Fig. 8: Experimental data of a bar lift, with parametric uncertainty in the grasping point of 20 cm. Same signals and conventions as in Fig. 7 Note the difference between the desired position and the reference one due to the parameter uncertainty. A stable behavior is achieved thanks to the compliance enabled by the control scheme.

our interest on the autonomous lifting part, which highlights the compliant behavior. The reference trajectory from the planner (dotted) is altered by the admittance (dashed) to accommodate the physical constraints of the system (via the estimated wrench). One can remark the good tracking performances of the low-level controller, as it follows effectively the trajectory provided by the admittance filter, with absolute error in position below 3 cm in $\mathbf{x}_W$ and $\mathbf{y}_W$, and below 14 cm for $\mathbf{z}_W$ (which can be explained by the safety cable weight) and absolute error in orientation below 2.1° along all axis, along all the trajectory. The maximal bar tilting angle θ_{bar} is also reached, indeed for the vertical configuration of the bar the position of the OTHex is the same along $\mathbf{x}_W$ independently from the grasping point, as visible in Fig. 8.

The second experiment devised to highlight the system

robustness consists in blocking the bar in its ascent. To do so, a rope is attached to the ground preventing the bar tilting angle to reach more than 18°. The wrench estimator is sensing an additional external force as soon as the rope is taut, see at the instant around 9 s in Fig. 9, with the same line convention as before. Once the ascent is blocked, a second compliance mechanism is triggered, the desired trajectory is 'waiting' for the measured trajectory to be in its vicinity. This mechanism consists in thresholding the error in the admittance filter to prevent unstable behavior due to excessive control action, which could be overcome either by adapting the admittance filter gain once the bar is blocked or by making the planner aware of tracking error as we did, thus avoiding tedious tuning of the admittance behavior. As it can be seen from the plot, the reaction to the blockage is smooth, and once the position error between the planned trajectory and the actual measurements is below a threshold, the behavior described in the nominal case is prevailing. This shows the robustness of our proposed solution to force
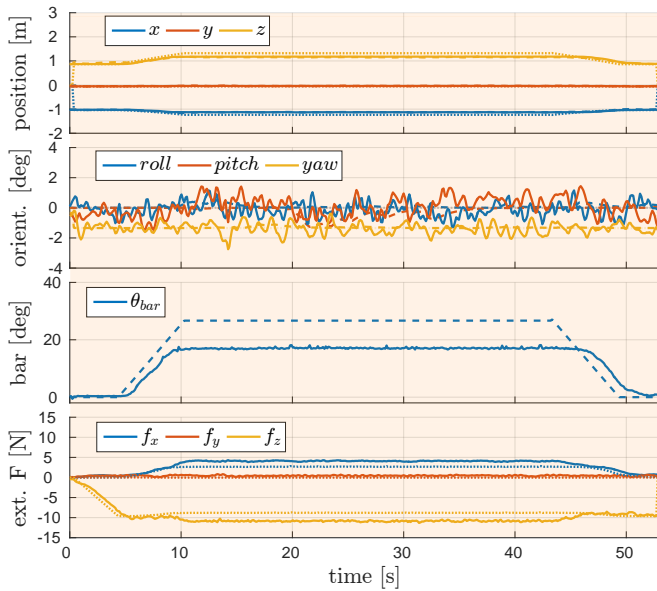
Fig. 9: Experimental data of a bar lift, blocked at $18°$ to emphasize the control framework compliance. Same signals and conventions as in Fig. 7. Note the difference between the desired position and the reference one coming from the admittance filter when the bar is blocked.

disturbances.

All three experiments recordings are regrouped in the associated multimedia video, which highlights our contributions and demonstrates its effectiveness in real case scenarios.

VII. CONCLUSION & FUTURE WORK

We introduced a new prototype of fully actuated Aerial Robot with a passive arm, that we called OTHex. This platform is capable of versatile manipulation task by fully exploiting its multi-directional thrust capability. Moreover, we show that for 'simple' manipulation task a passive arm is sufficient thus decreasing the system complexity and weight, allowing for higher endurance or payload and thus paving the way to the Flying Assistant usage. The design process was guided by experience gained on previous multi-directional thrust platform design, keeping the control allocation matrix balanced proved to maintain equivalent flight performances. Furthermore, our choice to rely on admittance filter is motivated by a more intuitive controller for contactless flight. The admittance typical inconsistencies for steady state commands with different virtual inertia were not encountered as we focused on smooth and gentle reaction. The main focus on our future work is toward increase of the system autonomy in general, we plan to increase the system decisional autonomy, by further developing the OTHex with on-board computer and refining the task planner policies, taking the wrench estimator into account, thus allowing agnostic cooperation with ground manipulator or human operator.

VIII. ACKNOWLEDGMENTS

REFERENCES

[1] A. Suarez, A. E. Jimnez-Cano, V. Vega, G. Heredia, A. R.-C. no, and A. Ollero, "Lightweight and human-size dual arm aerial manipulator," in *2017 Int. Conf. on on Unmanned Aircraft Systems*, Miami, FL, June 2017, pp. 1778–1784.

[2] M. Ryll, D. Bicego, and A. Franchi, "Modeling and control of FAST-Hex: a fully-actuated by synchronized-tilting hexarotor," in *2016 IEEE/RSJ Int. Conf. on Intelligent Robots and Systems*, Daejeon, South Korea, Oct. 2016, pp. 1689–1694.

[3] M. Tognon, B. Yüksel, G. Buondonno, and A. Franchi, "Dynamic decentralized control for protocentric aerial manipulators," in *2017 IEEE Int. Conf. on Robotics and Automation*, Singapore, May 2017, pp. 6375–6380.

[4] G. Antonelli, E. Cataldi, F. Arrichiello, P. Robuffo Giordano, S. Chiaverini, and A. Franchi, "Adaptive trajectory tracking for quadrotor MAVs in presence of parameter uncertainties and external disturbances," *IEEE Trans. on Control Systems Technology*, vol. 26, no. 1, pp. 248–254, 2018.

[5] A. Pumarola, A. Vakhitov, A. Agudo, A. Sanfeliu, and F. Moreno-Noguer, "PL-SLAM: real-time monocular visual SLAM with points and lines," in *2017 IEEE Int. Conf. on Robotics and Automation*, Singapore, May 2017, pp. 4503–4508.

[6] P. R. Soria, B. Arrue, and A. Ollero, "Detection, location and grasping objects using a stereo sensor on uav in outdoor environments," *Sensors*, vol. 17, no. 1, p. 106, Jan. 2017.

[7] R. Spica, P. Robuffo Giordano, M. Ryll, H. H. Bülthoff, and A. Franchi, "An open-source hardware/software architecture for quadrotor UAVs," in *2nd IFAC Work. on Res., Educ. and Develop. of Unmanned Aerial Systems*, Compiegne, France, Nov. 2013.

[8] M. Tognon, E. Cataldi, H. Tello Chavez, G. Antonelli, J. Cortés, and A. Franchi, "Control-aware motion planning for task-constrained aerial manipulation," *IEEE Robotics and Automation Letters, Special Issue on Aerial Manipulation*, 2018. doi: 10.1109/LRA.2018.2803206

[9] M. Tognon, C. Gabellieri, L. Pallottino, and A. Franchi, "Aerial co-manipulation with cables: The role of internal force for equilibria, stability, and passivity," *IEEE Robotics and Automation Letters, Special Issue on Aerial Manipulation*, 2018. doi: 10.1109/LRA.2018.2803811

[10] M. Gassner, T. Cieslewski, and D. Scaramuzza, "Dynamic collaboration without communication: Vision-based cable-suspended load transport with two quadrotors," in *2017 IEEE Int. Conf. on Robotics and Automation*, Singapore, May 2017, pp. 5196–5202.

[11] M. Tognon and A. Franchi, "Dynamics, control, and estimation for aerial robots tethered by cables or bars," *IEEE Trans. on Robotics*, vol. 33, no. 4, pp. 834–845, 2017.

[12] N. Staub, M. Mohammadi, D. Bicego, D. Prattichizzo, and A. Franchi, "Towards robotic MAGMaS: Multiple aerial-ground manipulator systems," in *2017 IEEE Int. Conf. on Robotics and Automation*, Singapore, May 2017.

[13] A. Franchi, R. Carli, D. Bicego, and M. Ryll, "Full-pose tracking control for aerial robotic systems with laterally-bounded input force," *IEEE Trans. on Robotics*, 2018. doi: 10.1109/TRO.2017.2786734

[14] M. Ryll, G. Muscio, F. Pierri, E. Cataldi, G. Antonelli, F. Caccavale, and A. Franchi, "6D physical interaction with a fully actuated aerial robot," in *2017 IEEE Int. Conf. on Robotics and Automation*, Singapore, May 2017, pp. 5190–5195.

[15] M. Tognon and A. Franchi, "Omnidirectional aerial vehicles with unidirectional thrusters: Theory, optimal design, and control," *IEEE Robotics and Automation Letters*, 2018. doi: 10.1109/LRA.2018.2802544

[16] B. Yüksel, C. Secchi, H. H. Bülthoff, and A. Franchi, "Reshaping the physical properties of a quadrotor through IDA-PBC and its application to aerial physical interaction," in *2014 IEEE Int. Conf. on Robotics and Automation*, Hong Kong, China, May. 2014, pp. 6258–6265.

[17] S. Rajappa, M. Ryll, H. H. Bülthoff, and A. Franchi, "Modeling, control and design optimization for a fully-actuated hexarotor aerial vehicle with tilted propellers," in *2015 IEEE Int. Conf. on Robotics and Automation*, Seattle, WA, May 2015, pp. 4006–4013.

[18] B. Yüksel, C. Secchi, H. H. Bülthoff, and A. Franchi, "A nonlinear force observer for quadrotors and application to physical interactive tasks," in *2014 IEEE/ASME Int. Conf. on Advanced Intelligent Mechatronics*, Besançon, France, Jul. 2014, pp. 433–440.

[19] A. Franchi and A. Mallet, "Adaptive closed-loop speed control of BLDC motors with applications to multi-rotor aerial vehicles," in *2017 IEEE Int. Conf. on Robotics and Automation*, Singapore, May 2017.